Accepted Manuscript

Title: Difluoroboron β-diketonate dye with intense red/near-infrared fluorescence in solutions and solid states

Authors: Nan Liu, Peng-Zhong Chen, Jian-Xin Wang, Li-Ya Niu, Qing-Zheng Yang

PII: S1001-8417(19)30232-3
DOI: https://doi.org/10.1016/j.cclet.2019.04.058
Reference: CCLET 4951

To appear in: *Chinese Chemical Letters*

Received date: 26 March 2019
Revised date: 9 April 2019
Accepted date: 22 April 2019

Please cite this article as: Liu N, Chen P-Zhong, Wang J-Xin, Niu L-Ya, Yang Q-Zheng, Difluoroboron β-diketonate dye with intense red/near-infrared fluorescence in solutions and solid states, *Chinese Chemical Letters* (2019), https://doi.org/10.1016/j.cclet.2019.04.058

Communication

Difluoroboron β-diketonate dye with intense red/near-infrared fluorescence in solutions and solid states

Nan Liu, Peng-Zhong Chen, Jian-Xin Wang, Li-Ya Niu*, Qing-Zheng Yang

Key Laboratory of Radiopharmaceuticals, Ministry of Education, College of Chemistry, Beijing Normal University, Beijing 100875, China

* Corresponding author.
E-mail address*: niuly@bnu.edu.cn*

Graphical Abstract

We reported a difluoroboron β-diketonate dye that displays bright red/NIR fluorescence in both solutions and solid states.

ARTICLE INFO

Article history:
Received 26 March 2019
Received in revised form 10 April 2019
Accepted 16 April 2019
Available online

Keywords:
Difluoroboron β-diketonate
Near-infrared
Solid state emission
Bioimaging

ABSTRACT

Difluoroboron β-diketonate (BF_2bdk) complexes have attracted much attention due to their outstanding photophysical properties. However, BF_2bdk with near-infrared fluorescence usually suffer from emission quenching in solid state due to the π–π stacking in aggregation. Herein, we report a series of BF_2bdk dye exhibiting donor-acceptor (D-A) structure with the difluoroboron moiety acting as the electron acceptor and the aminonaphthalene as the electron donor. It processes intense molar extinction coefficient, large Stokes shift and strong fluorescence in red/NIR region in both solution and aggregations. It was used for NIR imaging in living cells.

Difluoroboron β-diketonate (BF_2bdk) complexes have attracted much attention in recent years due to their impressive properties [1-17], such as strong fluorescence in both solution and solid state, large molar absorption coefficients, two-photon excited fluorescence, mechanochromic luminescence and room temperature phosphorescence. Hence, their attractive performances have made them a research focus and these attributes make them have wide applications in various fields, including fluorescent and phosphorescence imaging and sensing [18, 19], organic light-emitting diodes (OLED) [20-22], and photodynamic therapy [23, 24].

The photoluminescence properties of BF_2bdks strongly depend on the nature of their substitutions at 4, 6-positions of dioxaborine ring. In general, BF_2bdks with aliphatic groups at both 4, 6-positions are nonfluorescent in visible region due to the limited molecular conjugation, while BF_2bdks bearing aryl groups at 4, 6-positions are usually emissive and show tunable emission spectra from visible to near infrared (NIR) region by

* Corresponding author.
E-mail address: niuly@bnu.edu.cn

modulation of structural properties of ligands. In particular, NIR emission (650–900 nm) has distinct advantages in bioimaging and biosensing [25-27], including low photodamage to biological samples, deep tissue penetration, and minimum interference from background autofluorescence in living biosystems. Accordingly, the development of BF_2bdk-based NIR fluorophore is highly desirable and valuable for bioapplications. However, among the most of the reported BF_2bdk complexes, there are only a few reports on the properties and applications of BF_2bdk complexes with intense red/near-infrared fluorescence. D'Ale´o *et al.* have developed a series of curcuminoid and hemicurcuminoid based BF_2bdk derivatives whose emission red-shifted to red/near-infrared region [28, 29]. However, such structures usually suffer from emission quenching in solid state due to the π–π stacking in aggregation. Herein, we report a BF_2bdk derivative **N1** that display bright NIR fluorescence in both solution and solid state. By linking naphthalene to the 6-position of dioxaborine ring, BF_2bdk complex displays a considerable degree of aromaticity and expands the π-conjugation, leading the absorption/emission wavelength to red shift. Introduction of electron-donating amino groups to the naphthalene ring further shifts their absorption and emission due to the intramolecular charge transfer (ICT) from the ligands to the electron deficient dioxaborine ring. On the other hand, upon modulation of electron-donating or -withdrawing substituents of the aromatic rings on the 4-position, we synthesized compound **N1-N4** and studied their optical properties in organic solvents and solid states.

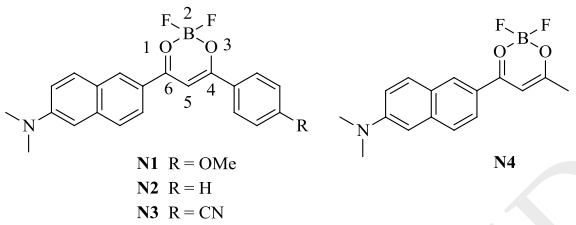

Scheme 1. Chemical structures of BF_2bdks **N1-N4**.

The synthetic routes of BF_2 complexes **N1–N4** are illustrated in Scheme 2. Firstly, the 6-amino-2-naphthoic acid methyl ester reacted with the methyl iodide to obtain *N, N′*-dimethyl groups. Then, the ketone precursors were deprotonated by NaH before reacting with the desired esters *via* the Claisen condensation reaction according to the literature. Finally, the BF_2 complexes **N1–N4** were easily prepared from the β-diketonate ligands **LN1–LN4** and BF_3/Et_2O in CH_2Cl_2. The target compounds **N1–N4** were characterized by ^{1}H NMR, ^{13}C NMR spectroscopy, high resolution mass spectrometry analysis.

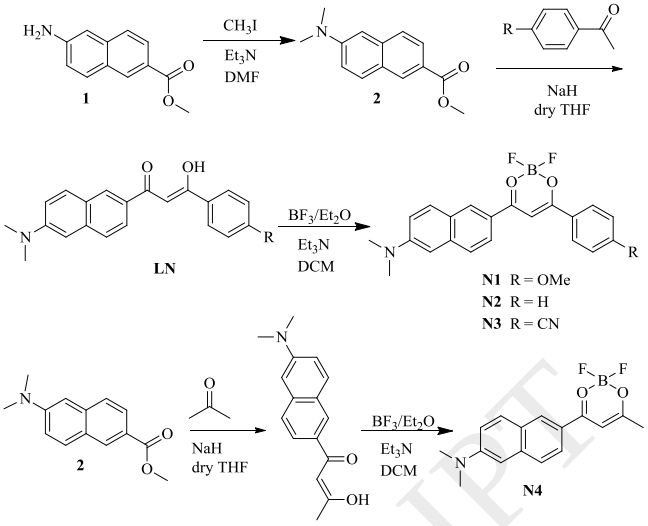

Scheme 2. Synthesis of **N1-N4**.

The complexes **N1–N4** are typical donor–acceptor (D-A) type fluorophores, with the difluoroboron moiety acting as the electron acceptor and the aminonaphthalene as the electron donor. The UV-vis absorption spectra for dyes **N1–N4** in different solvents are shown in Fig. S1 in Supporting information. All the spectra display relatively small absorption bands at λ_{max} < 400 nm, which are assigned to the π–π* transitions. The strong absorption bands ranging from λ_{max} = 455-559 nm has large molar extinction coefficient ($\varepsilon > 5\times10^4$ L mol^{-1} cm^{-1}). Such large ε, associated with the bathochromic shift of the lowest-energy transition band with the polarity of the solvent, is characteristic of an ICT. This process is confirmed by the equilibrium geometries of ground (S_n) state of **N1-N4** in gas phase which determined at B3LYP/6-31G level using DFT method (Fig. 1 and Fig. S2 in Supporting information). In all complexes, the HOMO and LUMO are mainly localized on aminonaphthalene and the dioxaborine ring, respectively, indicating ICT transition from the electron-donating aminonaphthalene units to electron-accepting dioxaborine ring. In addition, the longest absorption maxima are related to the electron-donating/withdrawing ability of the ligands. The absorption maxima of **N1-N3** with aryl groups show red-shift compared to **N4** in the same type solvent due to the expanded π-conjugation. The most red-shifted spectrum is obtained from the cyano analogues.

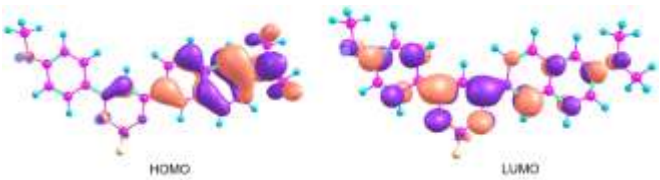

Fig. 1. Spatial distributions of the calculated HOMO and LUMO of **N1.** Calculations are based on ground state geometry by DFT at the B3LYP/6-31G* level.

The emission spectra of BF_2bdk complexes **N1–N4** in different solvents are provided in Fig. 2. All the chromophores display marked positive solvatochromism of their emission. The considerable bathochromic shifts in a polar solvent indicates enlarged dipoles and charge-transfer characteristics in their excited states. For instance, the overall emission bathochromic

shifts of **N1** is 143 nm from low-polarity toluene to high-polarity dimethyl sulfoxide (DMSO) (Table 1). Besides, the emission quantum efficiency also shows a strong dependence on the solvent's polarity (Table S1 in Supporting information). **N1-N4** display strong fluorescence with quantum yields > 90% in nonpolar or less polar solvents. For example, the QY of **N1** in toluene is close to unity (~95%). Upon increasing the solvent polarity, a marked decrease in the luminescence efficiency is observed, because ICT state is known to be able to go through nonradiative deactivation in polar solvents. The emission maxima of **N1-N3** are red shifted compared to the compound **N4** in the CH_2Cl_2, due to the larger π-conjugation systems. The introduction of different functional groups on the *para* position of phenyl ring has a significant effect on the emission properties of BF_2 complexes. The emission maxima of **N1**, **N2** and **N3** is 555, 573 and 582 nm in toluene. **N1** possesses ICT process in two directions (D-A-D type), which weakens the whole ICT process and is the possible reason for the blue-shifted emission. Compound **N3** with the largest D-A conjugation system displays the most red-shifted emission.

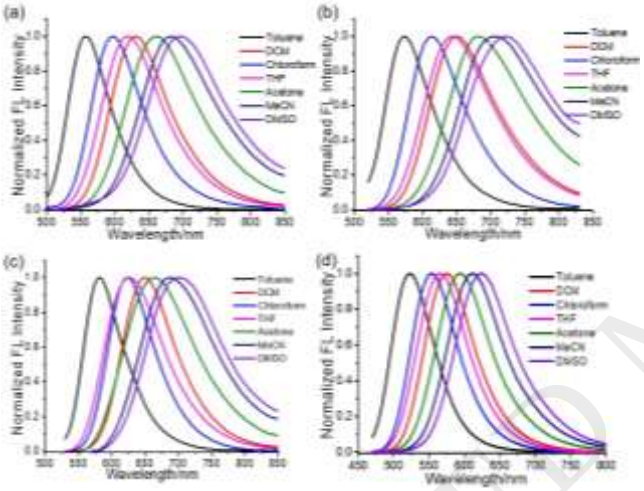

Fig. 2. Normalized fluorescence spectra of (a) **N1**, (b) **N2**, (c) **N3** and (d) **N4** in different solvents (1×10^{-5} mol/L).

Table 1
Photophysical data of **N1** in different solvents.

Solvents	λ_{abs} [a] (nm)	ε [b] (L mol^{-1} cm^{-1})	λ_{em} [c] (nm)	$\Delta\nu$ [d] (cm^{-1})	Φ_f [e]	τ_f [f] (ns)
Toluene	484	53400	555	2643	0.95	2.96
DCM	499	55800	631	4192	0.62	2.71
Chloroform	494	58800	596	3464	0.99	3.54
THF	486	60600	618	4395	0.52	2.68
Acetone	492	57900	660	5174	0.12	0.72
MeCN	496	41100	681	5477	0.01	0.42
DMSO	512	54600	698	5205	0.007	0.54

[a] Absorption maxima.
[b] Extinction coefficients calculated at the absorption maxima.
[c] Fluorescence emission maxima.
[d] Stoke shifts, $\Delta\nu$, were calculated using the equation $1/\lambda_{abs}-1/\lambda_{em}$.
[e] The absolute fluorescence quantum yields.
[f] Fluorescence lifetimes were measured with a EPLEDs (picosecond pulsed LEDs) light source and monitored at the emission maximum. All fluorescence lifetimes were fitted with single-exponential decays unless indicated.

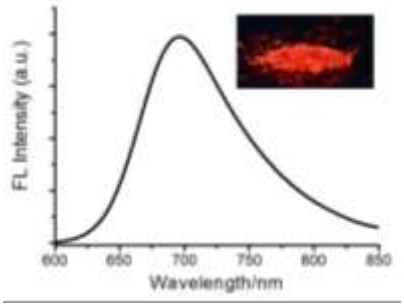

Fig. 3. Emission spectrum of **N1** in solid state. Inset: photograph of N**1** powder under UV lamp at 365 nm.

The emission properties of the chromophores **N1-N4** in the solid state are also investigated (Table S2 in Supporting information). The emission of the four complexes in solid state are located at 690-780 nm in the near-infrared region, significantly red-shifted compared to those in DCM solution, indicating strong intermolecular interactions between chromophores in solid state. Moreover, compound **N1** in solid state possesses the highest fluorescence quantum yield of 13% (Φ_f = 0.13). We assumes that a twist conformation would hamper the tight π–π stacking between the molecules in solid state.

In aqueous media, intrinsic hydrophobicity of aromatic structures of fluorophores will cause the formation of nanoaggregates. The bright fluorescence of **N1** in aggregates is a very attractive feature for applications in biological imaging. In addition, compound **N1** with large Stokes shift is of great advantage to avoid the interference from excitation and scattered light [30]. We examine the fluorescence imaging performance of **N1** in HeLa cells by using confocal laser scanning microscopy (CLSM). As shown in Fig. 4, after incubation with **N1** for 30 min, emission NIR channels are observed throughout the cytoplasmic area of the HeLa cells. The result indicates the NIR dye **N1** is able to be applied for NIR bioimaging.

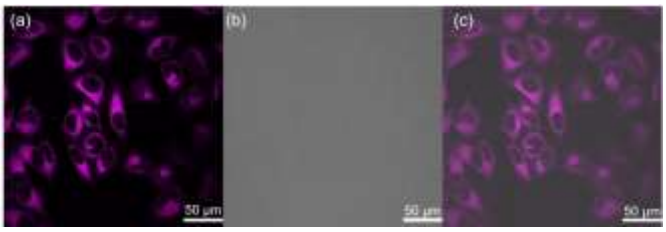

Fig. 4. CLSM images of HeLa cells incubated with **N1**. (a) NIR channel. (b) Bright field channel. (c) Overlay of (a) and (b).

In conclusion, we developed a new class of BF_2bdk-based dyes containing aminonaphthalene units with intense red/near-infrared fluorescence. They showed red-shifted absorption and emission spectra by introducing electron-withdrawing groups as the other ligand. Particularly, **N1** exhibited strong emission with quantum yield of 0.13 in solid state. It was successfully applied for NIR imaging in living cells. Possessing intense molar extinction coefficient, large Stokes shift, positive solvatochromism in different solvents and strong fluorescence in NIR region in aggregations, **N1** holds potential application as an environment sensitive probe in living systems.

Acknowledgment

This work was financially supported by National Natural Science Foundation of China (No. 21525206).

References

[1] P.Z. Chen, L.Y. Niu, Y.Z. Chen, Q.Z. Yang, Coord. Chem. Rev. 350 (2017) 196-216.
[2] D.H. Kim, A. D'Aléo, X.K. Chen, et al., Nat. Photonics 12 (2018) 98-104.
[3] X.F. Wang, H. Xiao, P.Z. Chen, et al., J. Am. Chem. Soc. (2019) DOI: 10.1021/jacs.9b00859
[4] G. Zhang, G.M. Palmer, M.W. Dewhirst, C.L. Fraser, Nat. Mater. 8 (2009) 747.
[5] W. Huang, X. Zhang, B. Chen, et al., Chem. Commun. 55 (2019) 67-70.
[6] Q. Jiang, M. Zhang, Z. Wang, et al., RSC Adv. 8 (2018) 30055-30060.
[7] L. Wilbraham, M. Louis, D. Alberga, et al., Adv. Mater. 30 (2018) 1800817.
[8] P.Z. Chen, H. Zhang, L.Y. Niu, et al., Adv. Funct. Mater. 27 (2017) 1700332.
[9] T. Liu, G. Zhang, R.E. Evans, et al., Chem.-Eur. J. 24 (2018) 1859-1869.
[10] P.Z. Chen, L.Y. Niu, H. Zhang, Y.Z. Chen, Q.Z. Yang, Mater. Chem. Front. 2 (2018) 1323-1327.
[11] P.Z. Chen, Y.X. Weng, L.Y. Niu, et al., Angew. Chem. Int. Ed. 55 (2016) 2759-2763.
[12] P.Z. Chen, J.X. Wang, L.Y. Niu, Y.Z. Chen, Q.Z. Yang, J. Mater. Chem. C 5 (2017) 12538-12546.
[13] K. Kamada, T. Namikawa, S. Senatore, Cet al., Chem.-Eur. J. 22 (2016) 5219-5232.
[14] M. Louis, R. Sethy, J. Kumar, et al., Chem. Sci. 10 (2019) 843-847.
[15] T. Butler, M. Zhuang, C.L. Fraser, J. Phys.Chem. C 122 (2018) 19090-19099.
[16] G.R. Krishna, M.S.R.N. Kiran, C.L. Fraser, U. Ramamurty, C.M. Reddy, Adv. Funct. Mater. 23 (2013) 1422-1430.
[17] G. Zhang, J. Chen, S.J. Payne, et al., J. Am. Chem. Soc. 129 (2007) 8942-8943.
[18] P. Zhang, Z.Q. Guo, C.X. Yan, W.H. Zhu, Chin. Chem. Lett. 28 (2017) 1952-1956.
[19] R.F. Wang, H.Q. Peng, P.Z. Chen, et al., Adv. Funct. Mater. 26 (2016) 5419-5425.
[20] Q. Liao, X.G. Wang, S. Lv, et al., ACS Nano 12 (2018) 5359-5367.
[21] C.T. Poon, D. Wu, V.W.W. Yam, Angew. Chem. Int. Ed. 55 (2016) 3647-3651.
[22] H.W. Mo, Y. Tsuchiya, Y. Geng, et al., Adv. Funct. Mater. 26 (2016) 6703-6710.
[23] B. Bai, C. Yan, Y. Zhang, Z. Guo, W.H. Zhu, Chem. Commun. 54 (2018) 12393-12396.
[24] K.S. Park, M.K. Kim, Y. Seo, et al., ACS Chem. Neurosci. 8 (2017) 2124-2131.
[25] W. Chen, Y. Pan, J. Chen, et al., Chin. Chem. Lett. 29 (2018) 1429-1435.
[26] P.Z. Chen, H.R. Zheng, L.Y. Niu, et al., Chin. Chem. Lett. 26 (2015) 631-635.
[27] Z. Guo, S. Park, J. Yoon, I. Shin, Chem. Soc. Rev. 43 (2014) 16-29.
[28] P.H. Lanoë, B. Mettra, Y.Y. Liao, et al., ChemPhysChem 17 (2016) 2128-2136.
[29] A. Felouat, A. D'Aléo, F. Fages, J. Org.Chem 78 (2013) 4446-4455.
[30] T.B. Ren, W. Xu, W. Zhang, et al., J. Am. Chem. Soc. 140 (2018) 7716-7722.